Theor Chem Acc (2005) 113: 63–68
DOI 10.1007/s00214-004-0611-2

Theoretical
Chemistry Accounts

Regular article

Structural and electronic trends in *ortho*-metalated dirhodium(II) complexes

Pipsa Hirva[1], **Pascual Lahuerta**[2], **Julia Pérez-Prieto**[3]

[1] Department of Chemistry, University of Joensuu, P.O. Box 11180101, Joensuu, Finland
[2] Departamento de Química Inorgánica, ICMOL, Universidad de Valencia, 46100, Burjassot, Valencia, Spain
[3] Departamento de Química Orgánica, ICMOL, Universidad de Valencia, 46100, Burjassot, Valencia, Spain

Received: 30 June 2004 / Accepted: 19 July 2004 / Published online: 22 November 2004

Abstract Properties of chiral dirhodium catalysts with *ortho*-metalated aryl phosphine ligands have been studied by a computational quantum chemical density functional theory method. The main aim in the current work was to systematically modify the ligand core of the $Rh_2(O_2C\ R)_2(PC)_2$ catalysts (PC is ortho-metalated aryl phosphine) in order to find structural and electronic trends involved with the modifications. The strongest impact on the properties of the active rhodium site was found when electron-withdrawing groups were introduced in the ligand core. The computational approach offers a possibility for a stepwise study of the properties of the catalysts and therefore a tool for further design of the most effective structures.

Keywords Dirhodium(II) catalysts – Phosphines – Quantum chemical calculations – Density functional theory method

1 Introduction

Dirhodium(II) tetracarboxylates have been found to be efficient in the catalytic transformation of α-diazo carbonyl compounds via dirhodium carbenoid species [1]. Ortho-metalated dirhodium(II) compounds with backbone chirality, $Rh_2(O_2C\ R)_2(PC)_2$ (PC is ortho-metalated aryl phosphine), have been studied in detail and represent a new family of dirhodium(II) catalysts that are also active and selective in cyclization reactions [2, 3, 4, 5]. The versatility of the ligands in these compounds allows control of the activity and enantioselectivity of the catalysts. Furthermore, since the backbone chirality creates different structural environment for ligands at the active axial site of the catalysts, the compounds form a group of promising candidates for a detailed computational study.

The $Rh_2(O_2C\ R)_2(PC)_2$ catalysts show a variation in activity and selectivity depending on the substituents introduced. Mainly two different ways of modifying the active center of the catalyst have been tried: (1) change of the carboxylate ligands and (2) introduction of substituents on the metalated phosphines. According to the results, change of carboxylates has a clear influence on the activity. While most of the catalysts are active in cyclopropanation reactions, those with electron-withdrawing groups, such as CF_3COO, are systematically more enantioselective and they are also the best candidates to induce C–H insertion. Though substituents on the phosphines also have catalytic influence, the best results are generally obtained with relatively basic and not very bulky triarylphosphines such as $P(C_6H_5)_3$ or $P(4\text{-}CH_3C_6H_4)_3$.

Current computational methods offer an alternative approach in the systematic search for the factors that would have the strongest impact on the catalyst behavior. The catalyst structure can be consistently altered, and the effect of the modulation on the structural parameters and energetics can give us valuable information on the trends in the properties of the active sites. After obtaining detailed knowledge on the steric and electronic properties of existing active catalysts, the design of more efficient and selective materials is facilitated.

Mononuclear rhodium catalysts have been widely studied by computational methods ranging from

Correspondence to: P. Hirva
E-mail: pipsa.hirva@joensuu.fi

molecular mechanics and semiempirical studies [6] to sophisticated density functional [7, 8, 9] and MP *x* [7, 10] computations. Modern quantum mechanical/molecular mechanics methods have also been applied in the study of larger mononuclear rhodium catalysts and reaction profiles [11, 12]. However, rhodium dimers have been the subject of only a few computational studies owing to the large size of the catalysts and the requirement of demanding methods to describe the metal–metal bonding in these systems. Most of them have focused on the tetrakis(carboxylato)dirhodium(II) catalyst in different applications, for example, molecular mechanics calculations on the origin of the regioselectivity in the C–H insertion reactions of dicarbonyl compounds [13] and on the dominant diastereomer in the cyclization of α-diazoesters [14]. Density functional theory (DFT) methods have been utilized in the study of the interaction of different axial ligands with the active rhodium site [15] and in the computation of the key steps in the Rh(II)-catalyzed cyclization of α-diazo ketoamides [16]. Recent studies by Nakamura and coworkers [17, 18] utilized density functionals and semiempirical PM3 in describing the C–H bond activation/C–C bond formation processes of diazoalkanes with dirhodium tetracarboxylate catalysts. Nowlan et al. [19] described the nature of the selectivity in rhodium-catalyzed cyclopropanation reactions by a hybrid density functional method, B3LYP.

The final aim of the work that is initiated in this paper is to confirm if the electronic and steric properties of the $Rh_2(O_2C\ R)_2(PC)_2$ catalysts can be predicted by DFT calculations and if these results could assist us in developing new, more active and selective catalysts. As a first step, we compare computational results for the key parameters of different catalyst structures, including existing and suitably tailored catalysts, to understand the effect of the modifications on the properties of the active catalytic sites.

2 Computational details

All calculations were carried out with the Gaussian98 program package [20]. DFT level of theory with the nonlocal density functional B3PW91 [21] was selected for the quantum chemical studies. The basis set comprised of the Stuttgart–Dresden effective small core potential augmented with an extra p-polarization function for rhodium [SDD(p)], and a standard all-electron basis set, 6-31G*, for other atoms. The system has been found to be reliable in the study of mononuclear platinum compounds [22], but we also tested it with a small dimeric rhodium compound $Rh_2(CO)_6(P(i\text{-}Pr)_3)_2$, for which the applied method was found to reproduce experimental [23] geometrical parameters accurately compared with several other methods and basis sets. Frequency analysis with no scaling was performed to ensure ground-state optimization. Natural population analysis [24] was used for obtaining the charge distribution for the models.

Full geometry optimization was performed for dimeric rhodium(II) catalysts of the type $Rh_2(O_2C\ R)_2(PC)_2$; *R* is H, CH_3, CF_3. The modification alternatives applied in this study are presented in Fig. 1. Water ligands were chosen for the axial positions to simplify the models and to avoid steric crowding in the ligand core at this point. Out of the four catalyst modifications considered here, *M*1 and *M*3 have been experimentally studied in catalyst reactions. *M*2 and *M*4 were designed to represent different electronic environments of the phosphines in order to reveal their effect in major structural parameters.

In addition to the phosphine complexes, we compared the trends in structural parameters of the tetrakis(carboxylato)dirhodium(II) catalysts [denoted as $Rh_2(O_2CR)_4$], which have been widely studied as precursors for many dirhodium(II) compounds.

An example of the accuracy of the fully optimized geometry of the catalysts compared with experimental values is listed in Table 1, where we have compared

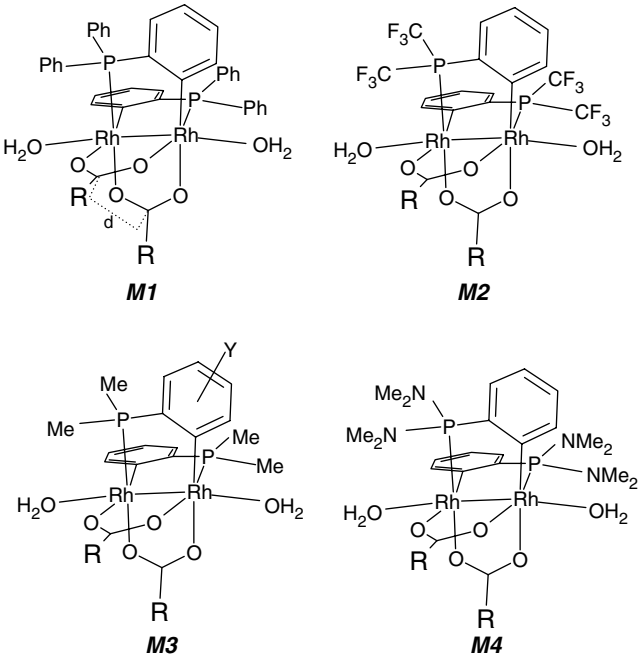

Fig. 1 Structural modifications for the ligand core of the *ortho*-metalated dirhodium(II) catalysts. Catalysts are denoted as *M1*, *M2*, *M3* and *M4*, depending on the type of phosphine, PC is PPh_3 (*M*1), $PPh(CF_3)_2$ (*M*2), $PPh(CH_3)_2$ (*M*3), and $PPh(N(CH_3)_2)_2$ (*M*4). Notations for other ligands: *R* is H, CH_3, CF_3; *Y* is NH_2, NO_2, CH_3, F

The basis set was obtained from the Extensible Computational Chemistry Environment Basis Set Database, version 9/12/01, as developed and distributed by the Molecular Science Computing Facility, Environmental and Molecular Sciences Laboratory which is part of the Pacific Northwest Laboratory, P.O. Box 999, Richland, WA 99352, USA, and funded by the US Department of Energy. The Pacific Northwest Laboratory is a multiprogram laboratory operated by Battelle Memorial Institue for the US Department of Energy under contract DE-AC06-76RLO 1830. Contact David Feller or Karen Schuchardt for further information.

Table 1 Comparison of selected computational[B3PW91//6-31G*, SDD(p) for rhodium] and experimental [25] structural parameters for the catalyst M3 (R = t-Bu). Bond distances are in Ångstroms and bond angle in degrees

Parameter	Comp	Exp	Diff	Diff%
r(Rh1–Rh2)	2.486	2.493	−0.007	−0.3
r(Rh1–P1)	2.227	2.190	0.037	1.7
r(Rh1–O1$_{carb}$)	2.159	2.172	−0.013	−0.6
r(Rh2–O2$_{carb}$)	2.202	2.180	0.022	1.0
r(O1–C1$_{carb}$)	1.267	1.240	0.027	2.2
r(O2–C1$_{carb}$)	1.265	1.240	0.025	2.0
r(Rh1–C$_{ort}$)	1.995	1.995	0.000	0.0
r(Rh1–O$_{H2O}$)	2.391	2.359	0.032	1.4
a(O1–C1–O2)	124.9	125.8	−0.900	−0.7
d(C1–C2)[a]	3.736	3.677	0.059	1.6

[a]Distance between carboxylate carbons

catalyst M3 including two axial water ligands (R is t-Bu) with a similar experimental crystal structure [25]. The optimized structure shows very reasonable agreement with the experimental bond lengths and angles, which allows consistent results on the structural trends upon modification of the ligand core.

3 Results and discussion

3. 1 Structural trends—effect of the carboxylate ligand

At the first stage, catalysts of the type $Rh_2(O_2C\ R)_2(PC)_2$, $M1$–$M4$, were modeled by changing the carboxylate ligand (Fig. 1). Two different ligands, CH_3COO and CF_3COO, were applied in order to explore the electronic effect of the carboxylates on the active rhodium site.

The most profound structural effect can be found on the Rh–Rh bond length (Fig. 2a). Although the difference in the Rh–Rh bond length is small (0.01–0.02 Å) in the phosphine catalysts, the trend in the modification is clear: substituting CH_3 with CF_3 leads to an increase in the metal–metal bond. The trend is consistent with experimental findings, for example, in catalyst $M1$ the difference between the two substitutions is 0.026 Å [2, 26].

A similar trend was found in Rh–O1$_{carb}$ (O1 is trans to phosphorus) bond lengths of the carboxylate groups (Fig. 2b): they are shorter for the acetate compounds than for the trifluoroacetate analogues. It should be noted that the other carboxylate oxygen, O2, which is trans to the *ortho*-metalated carbon, shows a similar trend, although the bond distances are somewhat longer owing to a different trans effect of the ligands. However, the Rh–O$_{H2O}$ bond distances of the axial water ligands show the opposite trend (Fig. 2e): they are consistently longer for the acetate compounds than for the trifluoroacetate analogues. Otherwise, changing the carboxylate ligand has no significant effect on the structural parameters of the ligand core surrounding the active site, as can be seen from the values of r(Rh–P) and r(Rh–C$_{ort}$) in Fig. 2c and d.

Especially, the shortening of the axial Rh–O$_{H2O}$ bond suggests that replacement of the acetate ligand by a by trifluoroacetate carboxylate ligand increases the strength of the interaction with compounds in the axial position, where the catalytic reactions are initiated.

Comparison of the structural changes in the simpler $Rh_2(O_2C\ R)_4$ systems gives a similar trend for the Rh–Rh and Rh–O$_{H2O}$ bond lengths. The Rh–O1$_{carb}$ distance, however, remains unchanged upon modification of the R ligand.

3.2 Structural trends—effect of phosphine

The structural trends for different phosphines are presented in Fig. 2. Modifying the phosphine ligands results

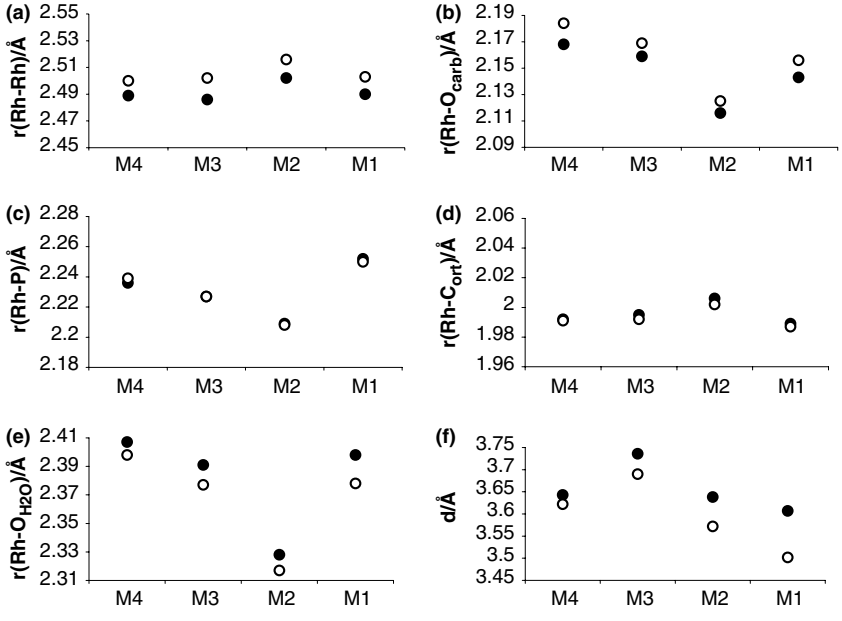

Fig. 2 The effect of modifying the carboxylate ligands on the selected bond lengths in catalysts $M1$, $M2$, $M3$ and $M4$. The catalysts are sorted in ascending order of the positive Rh charge (see Fig. 3). *Closed circles* represent CH_3-substituted carboxylates and *open circles* CF_3-substituted ones. The distance **d** in the last plot represents the distance between the central carbon atoms in the carboxylate ligands (Fig. 1).

in a large difference in Rh–P bond lengths, as can be expected. When the PPh_3 ligand is replaced with a less bulky $PPhMe_2$, the Rh–P bond decreases by 0.025 Å (experimentally by 0.02 Å). The Rh–P bond shortens even more when the phosphine is substituted with CF_3 groups instead of CH_3, as in *M*2. The following sequence can be established for the Rh–P bond distance: M1 > M4 > M3 > M2.

The modification of the phosphine also leads to a clear effect on the Rh–$O1_{carb}$ bond length, which changes more depending on the phosphine ligand than on the carboxylate ligand (Fig. 2b). The order of shortening the Rh–$O1_{carb}$ bond length follows the same order as the basicity of the phosphine, M4 > M3 > M1 > M2. Otherwise, the structural variation of the parameters is smaller, and *M*2 is the only one clearly differing from the other catalysts.

The distance between the active rhodium site and the axial water ligand shortens considerably in *M*2, compared with all other phosphines, which show very similar values. The role of the phosphine ligands is therefore also an important factor affecting the properties of the active site.

Additionally, the effect of phosphine changes the distance between the two carboxylate ligands (*d* in Fig. 1), which is 0.1–0.2 Å larger for catalyst *M*3 than for catalyst M1 and will result in a more open space between the carboxylate carbons thus facilitating the approach of bulkier axial ligands. The bulkier the ligands attached to the phosphine atom are, the smaller is the distance between the carboxylate carbons. Interestingly, the distance also decreases when the carboxylate ligand is changed from CH_3COO to CF_3COO. This indicates a strong steric effect involved with the phosphine catalysts, which can affect considerably the actual catalysis mechanisms.

3.3 Structural trends—effect of substituting the ortho-metalated ring

The importance of the electronic effects of the phosphines was further studied by calculating the structural changes with catalyst M3 using several substituents in the *ortho*-metalated phenyl rings (*Y* in Fig. 1). We applied a weakly electron withdrawing fluoride ligand, strongly electron withdrawing NO_2, weakly electron donating CH_3 and strongly electron donating NH_2 substituents in the 3- or 4- position of the phenyls. Table 2 compares selected structural parameters for nonsubstituted *M*3 catalyst with the corresponding Y-substituted catalysts. In all calculations, the carboxylate substituent R was hydrogen, which made the calculations faster without affecting the main results.

The effect of *Y*-substitution is relatively small and clear differences can only be found with the strongly electron withdrawing 4-NO_2 group. In a comparative test, this compound exhibits a significant decrease of the *ortho*-metalated Rh–C_{ort} bond length, a slight decrease in the Rh–O_{H2O} distance and no notable differences in the Rh–Rh and Rh–P distances. The effect is less pronounced for the compound with a 3-NO_2 group in the phosphine. The strongly electron donating NH_2 group results in the opposite behavior of the structural parameters. CH_3 and F are too weak to show any meaningful variation of the parameters. The results are consistent with experiments, since the effect of weak substituents has been found to be negligible for the ortho-metalated dirhodium catalysts [4a].

Table 2 Effect of substituted ortho-metalated phenyl ligands on selected structural parameters of catalyst M3(*R* = H), *Y* = 3-NH_2, 3-CH_3, H, 3-F, 3-NO_2 and 4-NO_2

	3-NH_2	3-CH_3	H	3-F	3-NO_2	4-NO_2
r(Rh1–Rh2)	2.492	2.493	2.495	2.493	2.499	2.498
r(Rh1–P1)	2.225	2.227	2.228	2.227	2.233	2.226
r(Rh1–C_{ort})	1.999	1.995	1.994	1.998	1.986	1.944
r(Rh1–O_{H2O})	2.389	2.384	2.383	2.376	2.362	2.355

3.4 Structural trends—effect of axial ligands

It has been suggested that one of the factors affecting the activity of the dirhodium(II) catalysts is the acidity of the active rhodium site [3]. To test the impact of the modification of the ligand core, we replaced one of the axial water ligands by ammonia, which induced several structural changes in the catalyst geometry (Table 3). The length of the axial bond Rh–*L* decreases substantially (0.12–0.17 Å), and as a result of the more basic nature of the NH_3 ligand, the substitution results in an increase in both the Rh–Rh bond length and the Rh–O_{H2O} distance of the opposite axial water ligand.

By comparing Rh–Rh and Rh–*L* bond lengths, it is clear that the longest Rh–Rh bond distance observed for M2 is accompanied by the shortest Rh–*L* bond distances, which indicates that strongly electron withdrawing groups in the phosphine ligands enhance the acidity of the active rhodium site, and hence lead to stronger interaction with basic axial ligands. The inductive effect of stronger interaction at the active site weakens the interaction at the opposite Rh site, thus facilitating the replacement of the remaining water ligand. However, there is a competing effect depending on the type of phosphines, the relative decrease in the Rh–*L* bond length and the increase in the Rh–O_B bond length is notably smaller for *M*2 than for *M*1 and *M*4, which suggests the more complex nature of the inductive effect from the ligand core.

In addition to the structural trends, the enhanced acidity of the active site can be seen in the interaction energy of ammonia when it replaces one of the axial water ligands. The energy values in Table 3 indicate enhanced acidity of the active site, when the phosphine ligands are substituted with electron-withdrawing CF_3 groups, as in the case of catalyst *M*2. Table 3 also shows

Table 3 The effect of axial ligands on theRh–Rh and Rh–*L* (*L* = NH_3 or OH_2) bond distances for $Rh_2(O_2C\ R)_2(PC)_2$ catalysts (*R* = CH_3). The notations in *parentheses* refer to the axial ligand at the active rhodium site (Rh1). The bond length Rh–O_B refers to the distance of the water ligand at the Rh2 site. ΔE-NH_3 (*R* is CH_3, CF_3) gives the energy of the replacementof one water ligand by ammonia for different carboxylates

	M4	M3	M2	M1
Rh–Rh(NH_3)	2.511	2.512	2.528	2.512
Rh–Rh(H_2O)	2.489	2.486	2.502	2.490
Rh–N(NH_3)	2.231	2.231	2.202	2.223
Rh–O_B(NH_3)	2.499	2.468	2.383	2.490
Rh–O(H_2O)	2.407	2.391	2.328	2.398
ΔE-NH_3 (CH_3) (kJ/mol)	−8.7	−9.6	−22.5	−10.3
ΔE-NH_3 (CF_3) (kJ/mol)	−14.9	−13.1	−26.2	−14.5

the effect of replacement of the acetate groups with trifluoroacetate, which further strengthens the interaction. The result is in agreement with the experimental findings that the replacement of CH_3COO with CF_3COO enhances the activity of dirhodium(II) catalysts [3, 4, 5].

3.5 Trends in charge distribution

We computed the charge distribution of the catalysts to see if the structural changes can be drawn directly from the changes of the charge distribution upon the modifications. Fig. 3 shows the natural population analysis charges for selected atoms around the active site.

Generally, the changes in the bond lengths are quite consistent with the changes in the natural populations of the corresponding atoms. Larger changes in the charges induce larger variation in the structural parameters. Obviously, the largest changes are connected with the ligands modified with electron-donating and electron-withdrawing groups, the phosphine and carboxylate ligands. Consistently with the structural changes, the largest electronic effect on the axial water ligand is introduced by changing the phosphine followed by a smaller change induced by the modification of the carboxylates. However, the inductive effect of the whole ligand core around the active site can have a different impact for the electronic nature of the active Rh site. Furthermore, electronic effects do not explain all the calculated structural trends. For example, in *M*1 the phosphorus charge *q*(P1) has a similar value as in *M*3, but the Rh–P bond length is considerably longer in *M*1. Also, according to the larger positive charge of rhodium in *M*1 we would expect a shorter bond length for the axial water ligand, but as seen in Fig. 2, the Rh–O_{H2O} bond is practically the same in *M*1 as in *M*3. Therefore, the steric properties of the ligand core will also play an important role in the nature of the active catalyst site. The computational approach will offer an effective tool to reveal the difference in the steric environment of the catalysts. This will also be the next step in our catalyst study.

4 Conclusions

In this work we performed quantum chemical density functional calculations on a series of dirhodium(II)

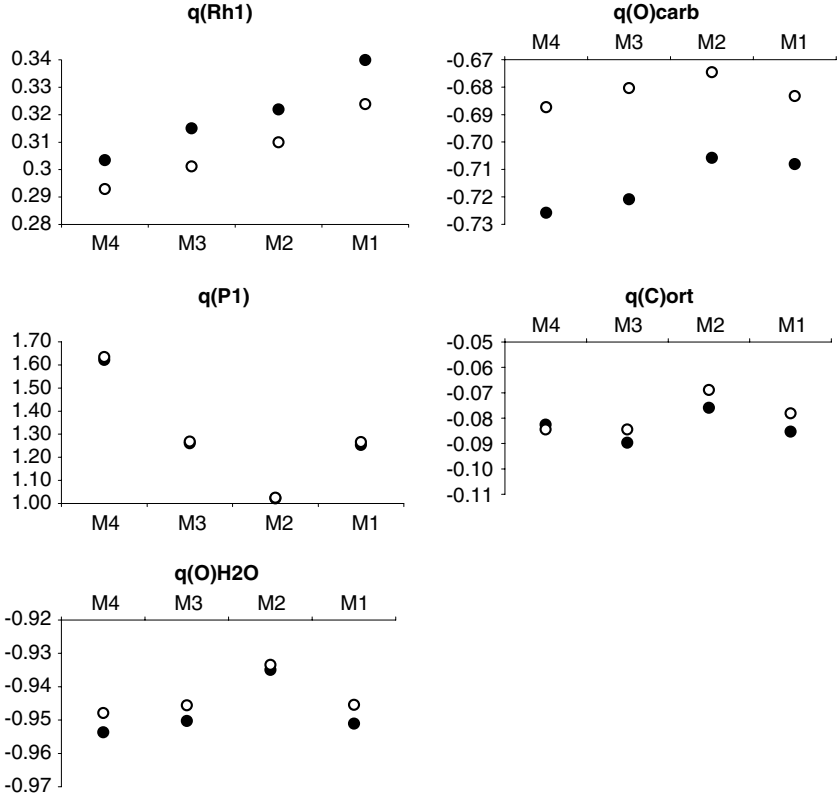

Fig. 3 The natural population analysis charges for selected atoms in different catalysts. Closed circles represent CH_3-substituted carboxylates and open circles CF_3-substituted ones

catalysts with *ortho*-metalated aryl phosphine ligands, in order to reveal structural and electronic trends involved with modification of the ligand core. The strongest electronic impact on the properties of the active Rh site could be obtained through a modification of the phosphine ligand with electron-withdrawing CF_3 groups. A smaller effect was induced by the carboxylate ligands, where the replacement of CH_3COO with CF_3COO resulted in a stronger interaction with the basic axial ligands, which can also be seen in the increase of the Rh–Rh distance of the catalyst. However, the structural trends could be interpreted to include steric effects on the interaction with the axial ligands. The less bulky phosphines and carboxylates were found to increase the distance between the central carbon atoms in the carboxylate ligands, thus opening the space for the approach of larger axial ligands. Our goal is to expand the computational approach on the relative importance of the steric and electronic properties in order to fully understand the role of the ligand structure in the enantiocontrol of the catalysts.

One advance in the application of computational methods is the possibility of systematically searching for the most efficient catalysts. Such a stepwise analysis is often experimentally difficult because of many competing electronic and steric effects involved in the reactions. Furthermore, small variations in the ligand structure lead to small differences in the structural trends, which might be impossible to reproduce experimentally. Although quantitatively accurate reaction energetics would require inclusion of solvent effects or the effect of neighboring molecules, qualitative trends in the structural parameters and energetics can assist in finding the factors that will have the largest influence on the properties of the active site.

References

1. (a) Doyle MP (1986) Chem Rev 86:919; (b) Doyle MP, Forbes DC (1998) Chem Rev 98:911; (c) Doyle MP, Catino AJ (2003) Tetrahedron Asymmetry 14:925; (d) Tsutsui H, Yamaguchi Y, Kitagaki S, Nakamura S, Anada M, Hashimoto S (2003) Tetrahedron Asymmetry 14:817; (e) Davies HML, Beckwith REJ (2003) Chem Rev 103:2861; (f) Davies HML, Townsend RJ (2001) J Org Chem 66:6595
2. Taber DF, Malcolm SC, Bieger K, Lahuerta P, Sanaú M, Stiriba S-E, Pérez-Prieto J, Angeles Monge M (1999) J Am Chem Soc 121:860
3. (a) Estevan F, Herbst K, Lahuerta P, Barberis M, Pérez-Prieto J (2001) Organometallics 20:950; (b) Estevan F, Lahuerta P, Pérez-Prieto J, Sanaú M, Stiriba S-E, Ubeda M (1997) Organometallics 16:880
4. Barberis M, Lahuerta P, Pérez-Prieto J, Sanaú M (2001) Chem Commun 439
5. Barberis M, Pérez-Prieto J, Herbst K, Lahuerta P (2002) Organometallics 21:1667
6. Surpateanu G, Agbossou F, Carpentier J-F, Mortreux A (1998) Tetrahedron Asymmetry 9:2259
7. Musashi Y, Sakaki S (2002) J Am Chem Soc 124:7588
8. Guiral V, Delbecq F, Sautet P (2001) Organometallics 20:2207
9. Tan KL, Bergman RG, Ellman JA (2002) J Am Chem Soc 124:3202
10. Hutschka F, Dedieu A, Eichberger M, Fornika R, Leitner W (1997) J Am Chem Soc 119:4432
11. Carbó JJ, Maseras F, Bo C, van Leeuwen PWNM (2001) J Am Chem Soc 123:123
12. Feldgus S, Landis CR (2001) Organometallics 20:2374
13. Doyle MP, Westrum LJ, Wolthuis WNE, See MM, Boone WP, Bagheri V, Pearson MM (1993) J Am Chem Soc 115:958
14. Taber DF, You KK, Rheingold AL (1996) J Am Chem Soc 118:547
15. Deubel DV (2002) Organometallics 21:4303
16. Padwa A, Snyder JP, Curtis EA, Sheehan SM, Worsencroft KJ, Kappe CO (2000) J Am Chem Soc 122:8155
17. Nakamura E, Yoshikai N, Yamanaka M (2002) J Am Chem Soc 124:7181
18. Yoshikai N, Nakamura E (2003) Adv Synth Catal 345:1159
19. Nowlan DT III, Gregg TM, Davies HML, Singleton DA (2003) J Am Chem Soc 125:15902
20. Frisch MJ, Trucks GW, Schlegel HB, Scuseria GE, Robb MA, Cheeseman JR, Zakrzewski VG, Montgomery JA Jr, Stratmann RE, Burant JC, Dapprich S, Millam JM, Daniels AD, Kudin KN, Strain MC, Farkas O, Tomasi J, Barone V, Cossi M, Cammi R, Mennucci B, Pomelli C, Adamo C, Clifford S, Ochterski J, Petersson GA, Ayala PY, Cui Q, Morokuma K, Malick DK, Rabuck AD, Raghavachari K, Foresman JB, Cioslowski J, Ortiz JV, Baboul AG, Stefanov BB, Liu G, Liashenko A, Piskorz P, Komaromi I, Gomperts R, Martin RL, Fox DJ, Keith T, Al-Laham MA, Peng CY, Nanayakkara A, Gonzalez C, Challacombe M, Gill PMW, Johnson B, Chen W, Wong MW, Andres JL, Gonzalez C, Head-Gordon M, Replogle ES, Pople JA (1998) Gaussian 98, revision A.7. Gaussian, Pittsburgh, PA
21. (a) Becke AD (1993) J Chem Phys 985648; (b) Perdew JP, Wang Y (1992) Phys Rev B 45:13244
22. Luzyanin KV, Haukka M, Bokach NA, Kuznetsov ML, Kukushkin VY, Pombeiro AJL (2002) J Chem Soc Dalton Trans 1882
23. Tomotake Y, Matsuzaki T, Murayama K, Watanabe E, Wada K, Onoda T (1987) J Organomet Chem 320:239
24. Glendening ED, Reed AE, Carpenter JE, Weinhold F NBO version 3.1
25. Morrison EC, Tocher DA (1991) J Organomet Chem 408:105
26. Chakravarty AR, Cotton FA, Tocher DA, Tocher JH (1985) Organometallics 4:8